EJN fens EUROPEAN JOURNAL OF NEUROSCIENCE

European Journal of Neuroscience, pp. 1–8, 2011 doi:10.1111/j.1460-9568.2011.07826.x

$Na_V1.1$ dysfunction in genetic epilepsy with febrile seizures-plus or Dravet syndrome

Linda Volkers,[1,2] Kristopher M. Kahlig,[3,*] Nienke E. Verbeek,[1,*] Joost H. G. Das,[1] Marjan J. A. van Kempen,[1] Hans Stroink,[4] Paul Augustijn,[5] Onno van Nieuwenhuizen,[6] Dick Lindhout,[1] Alfred L. George Jr,[3,7] Bobby P. C. Koeleman[1,*] and Martin B. Rook[2,*]

[1]Division of Biomedical Genetics, Department of Medical Genetics, University Medical Center Utrecht, Utrecht, The Netherlands
[2]Division Heart & Lungs, Department of Medical Physiology, University Medical Center Utrecht, Yalelaan 50, 3584 CM Utrecht, The Netherlands
[3]Department of Medicine, Vanderbilt University, Nashville, TN, USA
[4]Department of Neurology, Canisius-Wilhelmina Hospital, Nijmegen, The Netherlands
[5]SEIN – The Epilepsy Institutes of the Netherlands Foundation, Heemstede, The Netherlands
[6]Department of Pediatrics Neurology, University Medical Center Utrecht, Utrecht, The Netherlands
[7]Department of Pharmacology, Vanderbilt University, Nashville, TN, USA

Keywords: dravet syndrome, epilepsy, genetic epilepsy with febrile seizures-plus, human, *SCN1A*

Abstract

Relatively few *SCN1A* mutations associated with genetic epilepsy with febrile seizures-plus (GEFS+) and Dravet syndrome (DS) have been functionally characterized. In contrast to GEFS+, many mutations detected in DS patients are predicted to have complete loss of function. However, functional consequences are not immediately apparent for DS missense mutations. Therefore, we performed a biophysical analysis of three *SCN1A* missense mutations (R865G, R946C and R946H) we detected in six patients with DS. Furthermore, we compared the functionality of the R865G DS mutation with that of a R859H mutation detected in a GEFS+ patient; the two mutations reside in the same voltage sensor domain of $Na_v1.1$. The four mutations were co-expressed with β1 and β2 subunits in tsA201 cells, and characterized using the whole-cell patch clamp technique. The two DS mutations, R946C and R946H, were nonfunctional. However, the novel voltage sensor mutants R859H (GEFS+) and R865G (DS) produced sodium current densities similar to those in wild-type channels. Both mutants had negative shifts in the voltage dependence of activation, slower recovery from inactivation, and increased persistent current. Only the GEFS+ mutant exhibited a loss of function in voltage-dependent channel availability. Our results suggest that the R859H mutation causes GEFS+ by a mixture of biophysical defects in $Na_v1.1$ gating. Interestingly, while loss of $Na_v1.1$ function is common in DS, the R865G mutation may cause DS by overall gain-of-function defects.

Introduction

Genetic epilepsy with febrile seizures-plus (GEFS+) is a benign form of epilepsy in which patients have frequent febrile seizures early in childhood and later might develop epilepsy with afebrile seizures. Dravet syndrome (DS) or severe myoclonic epilepsy of infancy (SMEI; Singh *et al.*, 2001) is an intractable epilepsy syndrome, characterized by an onset of fever-induced generalized tonic–clonic or hemiclonic seizures within the first year of life, followed by other seizure types, slowing of development and mental disability in the majority of subjects. Absence of some of these features has also been described in what some call borderline SMEI (Fukuma *et al.*, 2004). Voltage-gated sodium channels are glycosylated complexes that are usually associated with one or two auxiliary β-subunits. Mutations in *SCN1A* (encoding the α-subunit $Na_V1.1$) and *SCN1B* (encoding the β1 subunit) have been linked to both GEFS+ and DS (Wallace *et al.*, 1998; Escayg *et al.*, 2000; Claes *et al.*, 2001; Patino *et al.*, 2009), with the majority of mutations found in *SCN1A* (Lossin, 2009). The majority of GEFS+ cases arise from missense mutations, which are distributed throughout the coding region. Functional analysis of some *SCN1A* missense mutations found in GEFS+ subjects exhibit a variety of biophysical defects that have been generalized as causing either gain-of-function or loss-of-function gating defects (Spampanato *et al.*, 2001, 2003, 2004; Lossin *et al.*, 2002, 2003; Barela *et al.*, 2006).

In DS, approximately half of the mutations are nonsense or frameshift alleles resulting in premature translation termination in *SCN1A*, which suggests that DS results from a complete loss of function of the mutant allele (Lossin, 2009). This hypothesis is supported by evidence from *Scn1a*-knockout mice (Yu *et al.*, 2006; Ogiwara *et al.*, 2007) and *SCN1A* gene deletions in DS patients (Suls

Correspondence: Dr Martin B. Rook, as above.
E-mail: m.b.rook@umcutrecht.nl

*K.M.K., N.E.V., B.P.C.K. and M.B.R. contributed equally to this work.

Received 17 May 2011, revised 30 June 2011, accepted 11 July 2011

et al., 2006). However, approximately one-third of the reported DS mutations are missense alleles. Functional studies demonstrated that a high proportion of missense mutations lead to nonfunctional sodium channels (Ohmori *et al.*, 2006). Nevertheless, a few studies have shown that some missense mutations produce functional channels and can either exhibit gain-of-function properties such as increased persistent current or loss-of-function effects such as decreased channel availability (Rhodes *et al.*, 2004; Ohmori *et al.*, 2006). The aim of this study was to investigate the electrophysiological properties of one GEFS+ and three DS associated missense mutations.

Materials and methods

Molecular SCN1A analysis

Genomic DNA was isolated from blood lymphocytes according to standard DNA isolation procedures. Genomic DNA was amplified by PCR and subsequently the entire coding region, including flanking regions of the exons, was analyzed by sequence analysis using automated sequence facilities (ABI3730; Applied Biosystems, Foster City, CA, USA). Sequence traces were analyzed using Mutation Surveyor software (SoftGenetics, LLC State College, PA, USA) using AB093548.1 as a reference.

Constructs

The *SCN1A* plasmid, which encodes the human neonatal $Na_v1.1$ ion channel, has previously been described (Lossin *et al.*, 2002). Mutations R859H, R865G, R946C or R946H were introduced by QuikChange site-directed mutagenesis (Stratagene, Cedar Creek, TX, USA) according to the manufacturer's protocol using the following primer pairs: sense 5′ GGAAGGATTATCTGTTCTCCATTCATTTCGATTGCTGCGAG 3′ and antisense 5′ CTCGCAGCAATCGAAATGAATGGAGAACAGA-TAATCCTTCC 3′ (exchange c.G2576A to obtain p.R859H), sense 5′ GTTCATTTCGATTGCTGGGAGTTTTCAAGTTGGC 3′ and antisense 5′ GCCAACTTGAAAACTCCCAGCAATCGAAATGAAC 3′ (exchange c.C2593G to obtain p.R865G), sense 5′ CTTCCTGATTG-TGTTCTGCGTGCTGTGTGGGG 3′ and antisense 5′ CCCCACA-CAGCACGCAGAACACAATCAGGAAG 3′ (exchange c.C2836T to obtain p.R946C) and sense 5′ CTTCCTGATTGTGTTCCACGT-GCTGTGTGGGGAG 3′ and antisense 5′ CTCCCCACACAGCACG-TGGAACACAATCAGGAAG 3′ (exchange c.G2837A to obtain p.R946H). All constructs were verified by sequencing.

Cell culture and transfections

Human-derived tsA201 cells were cultured in Dulbecco's modified Eagle's medium supplemented with FBS, 10% penicillin, 100 U/mL; streptomycin, 100 μg/mL; and L-glutamine, 0.05%; in a humidified incubator at 37 °C with 5% CO_2. Culture media and supplements were obtained from Biowhittaker, Vervier, Belgium. Transient transfections were performed with Lipofectamine (Invitrogen, Carlsbad, CA, USA) using in total 6 μg of $Na_v1.1$, $\beta1$ and $\beta2$ pDNAs in a ratio of 10 : 1 : 1, as previously described by Lossin *et al.*, 2002. Cells were incubated with CD8 positive beads (Invitrogen, Oslo, Norway) to identify $\beta1$-expressing cells; cells expressing $\beta2$ were identified with epifluorescence. Cells that expressed both β-subunits were used for electrophysiological recording experiments. All experiments were performed 48–72 h after transfection. For electrophysiological measurements at least two different clones of either WT or mutant constructs were evaluated.

Electrophysiology

Prior to patching, cells were incubated for at least 1 h in cell culture medium containing (in mM) NMDG, 140; KCl, 4; $CaCl_2$, 1; $MgCl_2$, 1; Na_2HCO_3, 14.3; HEPES, 15.1; Glucose, 17.5; with 1× amino acids (Gibco, Paisley, UK), 1 × non-essential amino acids (NEAA; Gibco, Paisley, UK; pH 7.35) supplemented with 10% FCS (Biowhittaker, Vervier, Belgium), penicillin 100 U/mL (Biowhittaker, Vervier, Belgium), streptomycin 100 U/mL (Biowhittaker, Vervier, Belgium) and 2 mM L-glutamine (Biowhittaker, Vervier, Belgium) in a humidified atmosphere at 37 °C, 5% CO_2. For patch experiments, cells were bathed in modified Tyrode's solution containing (in mM) NaCl, 140; KCl, 5.4; $CaCl_2$, 1.8; $MgCl_2$, 1; glucose, 6; and HEPES, 6; (pH adjusted to 7.4 with NaOH). Sodium currents were measured at room temperature (20–22 °C) using the whole-cell voltage-clamp configuration with an Axopatch 200B amplifier (Axon Instruments, Union City, CA, USA). Patch electrodes were pulled from borosilicate glass capillaries and fire-polished. Pipettes were fabricated with a micropipet puller (Sutter Instruments, Novato, CA, USA) and had a resistance of 1.5–2.2 MΩ when filled with the following intracellular solution (in mM): NaF, 10; CsF, 110; CsCl, 20; EGTA, 2; and HEPES, 10; (pH 7.35). Cells were allowed to stabilize for 10 min after the whole-cell configuration was established. Cells that had a sodium current of < -600 pA were excluded from analyses to avoid contamination by endogenous currents. Cells expressing sodium current > -6000 pA were excluded from analyses to avoid recordings with poor voltage control. Cell capacitance and pipette series resistance were compensated for by 90%. Leak currents were subtracted using a $P/4$ procedure. Currents were acquired with a low-pass filter of 10 kHz and digitized at 100 kHz. For analysis, the recorded currents were low-pass-filtered at 5 kHz. The voltage-clamp protocols were generated using pCLAMP9.2 (Axon Instruments). Steady state of activation and channel availability were determined by fitting the data with a single Boltzmann $y = I_{max}/(1 + \exp((1/k) \times (V - V_{½})))$, where V is the variable conditioning potential, $V_{½}$ the voltage of half-maximal activation, k the slope and I_{max} the normalized maximal amplitude of the Boltzmann current. The recovery from inactivation was analyzed by fitting the data with a double exponential function $I/I_{max} = A_{fast} \times (1-\exp(-t/\tau_{fast})) + A_{slow} \times (1-\exp(-t/\tau_{slow})) + C$, where τ_{fast} and τ_{slow} denote a fast and a slow time constant, A_{fast} and A_{slow} represent the two fractional amplitudes and C is the level of noninactivating sodium current. Speed of inactivation was evaluated by fitting the decay phase of the sodium current with a double exponential function $I/I_{max} = A_{fast} \times \exp(-t/\tau_{fast}) + A_{slow} \times \exp(-t/\tau_{slow}) + C$, where the parameters are defined as above. Persistent sodium current was measured in the final 10 ms of a 100 ms depolarizing pulse to −20, −10 and 0 mV, and determined by subtracting background current measured in the presence of 10 μM tetrodotoxin (Alomone, Jerusalem, Israel) from tetrodotoxin-free records. Data analysis was performed using Excel 2008 (Microsoft, Seattle, WA, USA) and Origin Pro 8.0 (Microcal, Northhampton, MA, USA) and Kaleidagraph 4.0 (Synergy Software, Reading, PA, USA) software. Values are expressed as means ± SEM. Statistical comparison was done using an unpaired Student's t-test; a $P < 0.05$ value was considered significant.

Results

Clinical phenotypes

The novel R859H mutation was detected in a girl diagnosed with GEFS+ and a paternal history of (a)febrile seizures (Table 1). Her

TABLE 1. Clinical features of patients with an *SCN1A* mutation

SCN1A mutation	Gender	Age study (years)	Seizure onset	Seizure types	AEDs	Response to AED	Development	Ataxia	Epilepsy classification	Inheritance
R859H	F	8.5	13 months	GTCS, CPS	Currently no AEDs	Seizure-free	Normal	No	GEFS+	Paternal
R859H	M	29	1 years	GTCS	Currently no AEDs	Seizure-free	Normal	No	GEFS+	ND
R865G	M	9.5	9 months	H, Mc, CPS	VPA, LTG, LEV	Seizure-free	Severely delayed	No	Dravet	ND
R946C	F	5.5	10 months	GTCS	VPA	Intractable	Moderately delayed	Yes	Dravet	de novo
R946H	M	24	< 1 years	GTCS, Mc, CPS	VPA, TPM	Intractable	Delayed	Unknown	Dravet	ND
R946H	M	4.5	4 months	GTCS, H	VPA, TPM	Intractable	Delayed	Unknown	Dravet	ND
R946H	F	3	10 months	GTCS, Mc, A, MAs	VPA, LEV, CLZ	Intractable	Delayed	Unknown	Dravet	ND

A, atypical absences; AED, antiepileptic drug; CLZ, clonazepam; CPS, complex partial seizure; GTCS, generalized tonic–clonic seizures; H, hemi convulsions; LEV, levetiracetam; LTG, lamotrigine; MAs, myoclonic–astatic seizures; Mc, myoclonias; ND, not determined; TPM, topiramate; VPA, valproate.

febrile convulsions, generalized tonic–clonic seizures (GTCS), started at the age of 13 months after a diphtheria/tetanus/whole cell pertussis/inactivated poliovirus (DTwcP-IPV) and haemophilus influenzae type b (Hib) vaccination and were recurrent and often prolonged. After the age of 3.5 years she also experienced afebrile GTCS and an isolated complex partial seizure (CPS). Electroencephalography (EEG) demonstrated bilateral occipital–temporal spike-wave complexes and a few predominantly left-sided isolated occipital spike-waves. The patient responded well to valproate (VPA). Her last seizure was reported at age 5.5 years and EEG analysis at the age of 6 years did not show epileptiform activity. She had normal development except for some features of attention deficit–hyperactivity disorder (ADHD). Her father experienced approximately ten febrile seizures between age 1 and 6 years. In the next 9 years, he experienced approximately five afebrile seizures. He received VPA from age 11 years until he was 17 years old. The family history of first-degree relatives was negative for febrile and afebrile seizures.

The novel R865G mutation was detected in a boy who had right-sided hemiconvulsions with postictal hemiparesis since the age of 9 months (Table 1). He also experienced myoclonic jerks and CPS. His EEGs showed a near-normal background pattern with isolated sharps and sharp waves in both hemispheres. He was diagnosed with DS. Magnetic resonance brain imaging was normal. At the age of 60 months, he was deemed to have a severe developmental delay with a developmental age of 29 months. After addition of levetiracetam (LEV) to VPA and lamotrigine (LTG) at the age of 6.5 years he is seizure-free to date. His family history was negative for febrile convulsions and epilepsy. His parents are consanguineous. DNA analysis of the parents was not available.

The R946C mutation was previously found in subjects with DS, but not functionally characterized. We also detected this mutation in a girl diagnosed with DS. She experienced her first seizure at age 10 months, after a vaccination against DTwcP-IPV and Hib. The majority of her seizures were fever-provoked GTCS. VPA monotherapy controlled her seizure frequency to twice a year. She showed ataxia and a moderate developmental delay. Her IQ was 60 at the age of 5.5 years (Table 1).

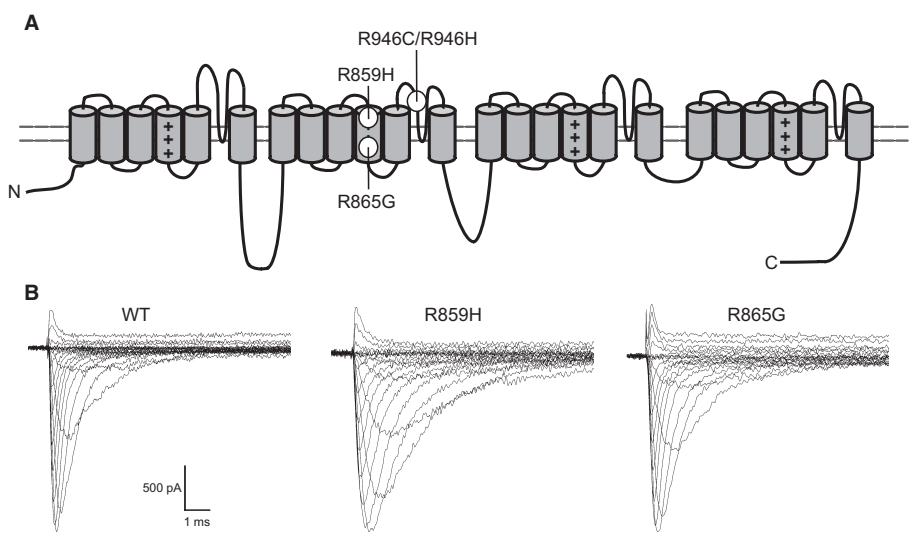

FIG. 1. Mutation location and representative WT and mutant $Na_v1.1$ whole-cell currents. (A) Schematic representation of the $Na_v1.1$ channel. The S4 voltage sensors are marked with plus signs (+). The locations of the mutations are as depicted. (B) Assembled sodium currents elicited by increasingly depolarizing pulses. Representative sodium currents recorded from tsA201 cells expressing WT, R859H or R865G ion channels in combination with $\beta1$ and $\beta2$ subunits. Currents were activated by depolarizing voltage steps ranging from −80 mV to +90 mV in increments of 5 mV. Both mutants produced functional sodium currents, which were similar in amplitude to WT currents (Student's *t*-test: WT $n = 13$; R859H $n = 12$, $P = 0.89$; R865G $n = 10$, $P = 0.97$). See Materials and Methods and inset Fig. 2B for pulse protocol.

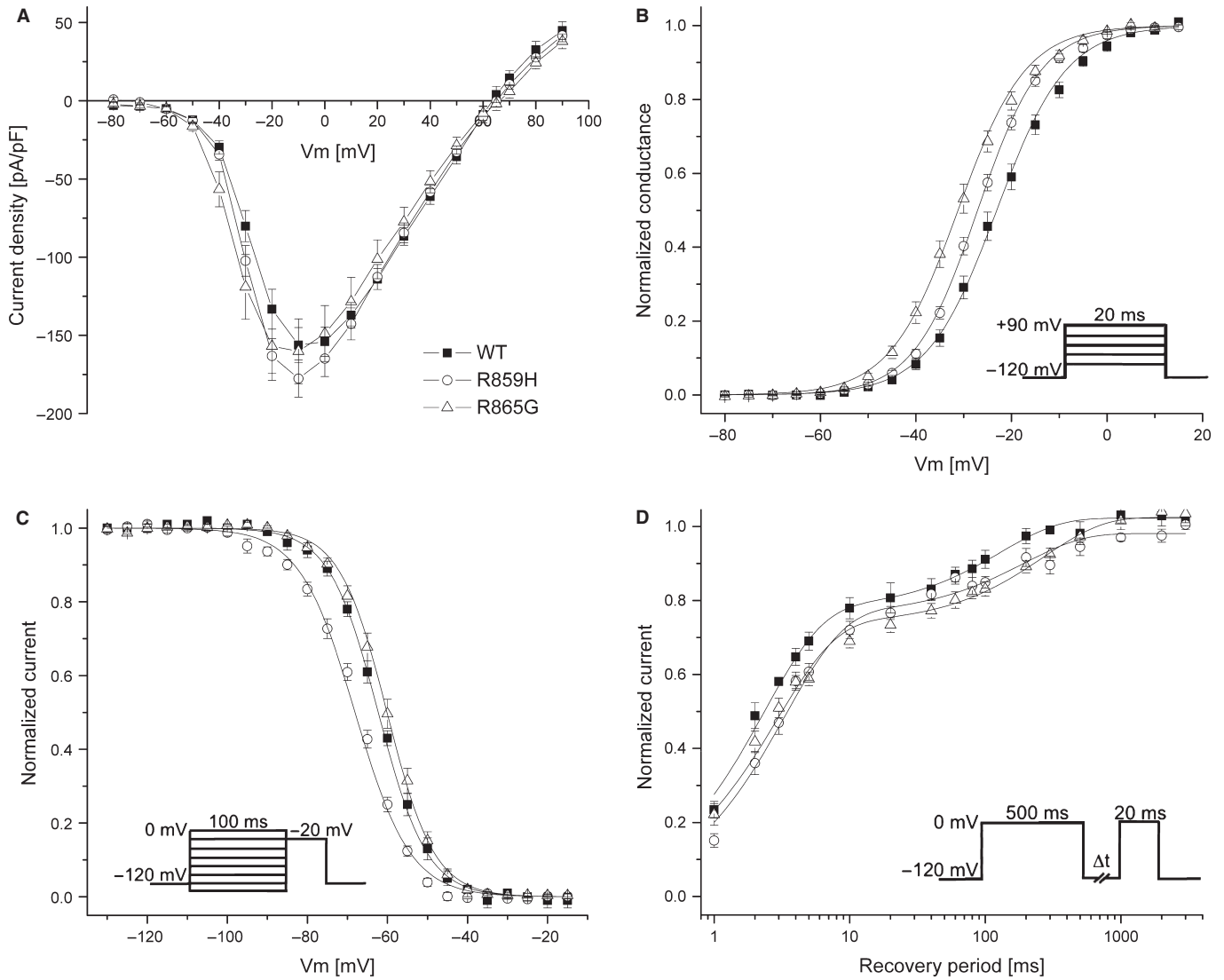

FIG. 2. *SCN1A* mutations alter gating of $Na_v1.1$ channels. (A) Current–voltage relationships for $Na_v1.1$ WT, R859H and R865G. Whole-cell currents were normalized to cell capacitance and plotted against the test potentials. WT and mutant channels produce similar peak current densities. (B) Voltage dependence of activation was determined by measuring peak currents during variable test pulses from a holding potential of −120 mV. The currents were divided by the electrochemical driving force and normalized to the maximum peak current to obtain the normalized sodium conductance. Both mutants exhibited a negative shift in the voltage dependence of activation, resulting in a gain-of-function of activation (Student's *t*-test, WT $n = 13$; R859H $n = 12$, $P = 0.004$; R865G $n = 10$, $P < 0.0001$). (C) Voltage dependence of inactivation (voltage dependence of channel availability) was measured using a two-step pulse protocol (inset) by applying inactivating prepulses from −140 to −10 mV in 5 mV steps. Currents at the −20 mV test pulse were normalized to the peak current amplitude at the beginning of each prepulse and plotted against the prepulse potential. The voltage dependence of inactivation of R859H channels showed a hyperpolarized shift, causing a loss of channel availability at potentials more negative than −40 mV (Student's *t*-test, WT $n = 8$; R859H $n = 6$, $P = 0.0003$). (D) Recovery from fast inactivation was acquired by applying a 500 ms inactivating prepulse to the cell followed by a −120 mV step for variable time durations (1–3000 ms) to allow channel recovery, then a 20 ms test pulse to 0 mV. Fractional recovery was calculated by dividing the maximum peak current of the test pulse by the maximum current amplitude of the corresponding conditioning pulse. The data were fitted with a double exponential function. Both mutants showed a slower recovery from inactivation than WT (Student's *t*-test, WT $n = 5$; R859H, $n = 7$, $P = 0.02$; R865G, $n = 9$, $P = 0.0002$).

TABLE 2. Biophysical parameters of $Na_v1.1$ WT and mutant ion channels

	Voltage dependence of activation			Voltage dependence of inactivation			Recovery from fast inactivation				
	$V_{½}$ (mV)	k	n	$V_{½}$ (mV)	k	n	τ_{fast} (ms)	A_{fast} (%)	τ_{slow} (ms)	A_{slow} (%)	n
Nav1.1 WT	−23.1 ± 1.1	7.3 ± 0.3	13	−62.3 ± 0.9	−6.1 ± 0.3	8	2.3 ± 0.2	77 ± 3	130 ± 11	25 ± 2	5
R859H	−27.1 ± 0.6†	6.7 ± 0.2	12	−68.1 ± 0.7†	−6.9 ± 0.3	6	3.3 ± 0.3*	76 ± 1	191 ± 25*	22 ± 2	7
R865G	−31.2 ± 1.1‡	7.1 ± 0.3	10	−60.1 ± 0.9	−5.9 ± 0.1	10	2.9 ± 0.3	71 ± 5	207 ± 12*	29 ± 4	9

Values presented are mean ± SEM. Values significantly different from $Na_v1.1$ WT are indicated as follows: *$P < 0.05$, †$P < 0.001$, ‡$P < 0.0001$.

The R946H mutation was previously described in five patients with DS and one subject with partial epilepsy with antecedent febrile seizures (Fukuma *et al.*, 2004; Berkovic *et al.*, 2006; Harkin *et al.*, 2007, Depienne *et al.*, 2009; Liao *et al.*, 2010). Functional analysis of this mutation showed complete loss of function of the mutant allele (Liao *et al.*, 2010). We also detected the R946H mutation in three unrelated subjects diagnosed with DS (Table 1).

The first case was an adult male who had GTCS, initially provoked by DTwcP-IPV vaccination followed by fever, in his first year of life. Subsequently, he developed myoclonias and complex partial seizures. He experienced monthly seizures while receiving a combination of VPA and topiramate (TPM), and exhibited a moderate developmental delay.

The second case was a boy who had his first seizure after a DTwcP-IPV and Hib vaccination at age 4 months (Table 1). Initially the clonic component of the seizures (focal/hemiconvulsions) did not involve all limbs. Later on he developed GTCS, often occurring in clusters and provoked by fever. At age 1.5 years a developmental delay became evident. His interictal EEG was normal until age 3 years, rapidly followed by diffusely disturbed EEGs later in life. After replacement of the combination of VPA and LTG by VPA and TPM, seizure frequency was reduced.

The third patient was a girl who experienced her first GTCS at age 10 months, and subsequently developed myoclonias, atypical absences and myoclonic–astatic seizures previously described by Verbeek *et al.*, 2011;. Her EEG at the age of 3 years showed multifocal (poly)spike–wave complexes. VPA, LEV and clonazepam (CLZ) administration reduced seizures to two per month. She also showed developmental delay, with a developmental age of 18 months at the age of 2.5 years (Table 1). Her deceased father had been diagnosed with DS with a milder phenotype (Verbeek *et al.*, 2011). Unfortunately, DNA of the father and the paternal grandparents was not available for analysis.

R946C and R946H channels were nonfunctional

The two missense mutations, R946C and R946H, are located in the $Na_v1.1$ domain II pore-loop (Fig. 1A). When co-expressed with the β1- and β2-subunits, neither mutant channel produced measurable sodium currents. Our findings for R946H are in agreement with recent observations made by Liao *et al.* (2010). The observation that R946C also leads to a complete loss of ion channel function suggests that R946 is a residue critical for $Na_v1.1$ function.

R859H and R865G exhibited gating defects

The two novel *SCN1A* mutations located in the voltage-sensing S4 segment of domain II, R859H and R865G, both produced functional sodium channels and were further examined (Fig. 1B). Compared to wild-type (WT) channels, R859H and R865G exhibit similar peak current densities (R859H $t_{23} = 0.14$, $P = 0.89$; R865G $t_{21} = 0.03$, $P = 0.97$; Fig. 2A). Voltage-dependence of activation was altered for both mutant channels. Half-maximal voltage ($V_{½}$) for activation was shifted towards more hyperpolarized potentials (R859H −4 mV, $n = 12$; R865G −8.1 mV, $n = 10$; Table 2) compared to WT channels (R859H $t_{23} = 3.21$, $P = 0.004$; R865G $t_{21} = 5.27$, $P < 0.0001$; Fig. 2B and Table 2), resulting in a gain-of-function for both mutants albeit more prominent for R865G. The $V_{½}$ of inactivation was shifted towards more negative values for the R859H mutant channels (−5.8 mV, $n = 6$), while the R865G mutant was similar to WT channels (R859H $t_{12} = 4.94$, $P = 0.0003$; R865G $t_{16} = -1.81$, $P = 0.09$; Fig. 2C and Table 2). This loss-of-function gating defect for R859H suggests a reduction in channel availability at potentials more negative than −40 mV. To investigate the recovery from inactivation, we applied a 500 ms depolarizing prepulse to inactivate all ion channels, followed by a −120 mV step of increasing durations (1–3000 ms) to allow the channels to recover from inactivation, followed by a depolarizing test pulse. The fractional recovery from inactivation with time was calculated by dividing the maximum peak current elicited by the test pulse by the peak currents obtained at the conditioning pulse. The data was fitted with a double exponential to obtain a fast (τ_{fast}) and a slow (τ_{slow}) recovery from inactivation constant. Both mutant channels exhibited a similar slowing in the recovery from fast inactivation (Fig. 2D) indicated by a larger time

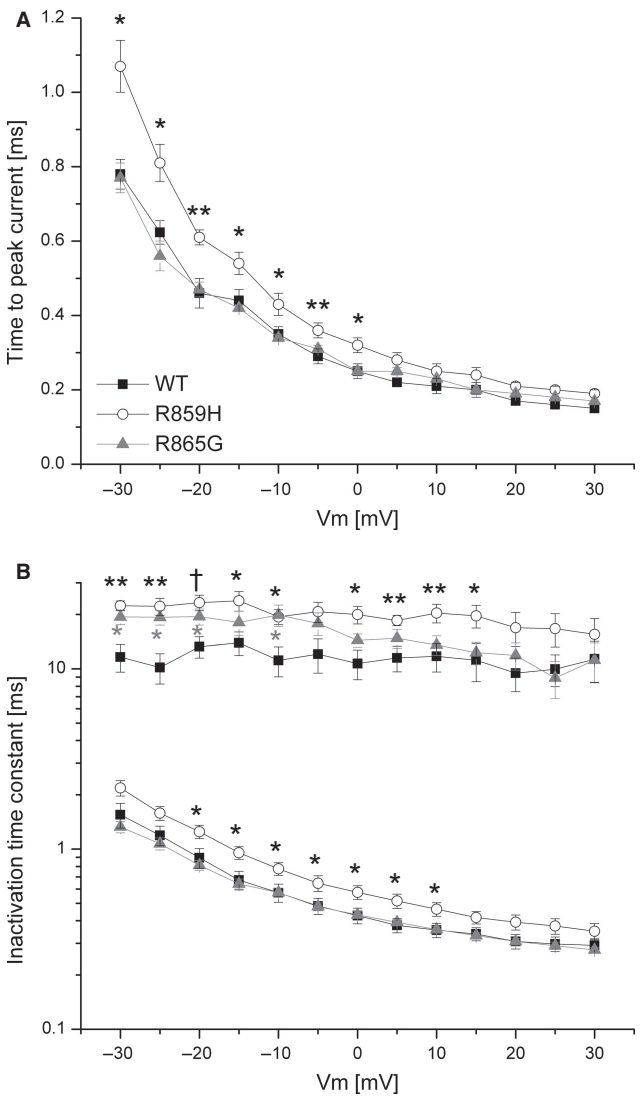

FIG. 3. Mutant channels exhibited time-dependent gating defects. (A) Time to peak current was analyzed from −30 to +30 mV. R859H exhibited a significantly delayed activation time in the voltage range −30 to +5 mV compared to $Na_v1.1$ WT (Student's *t*-test, WT $n = 13$; R859H $n = 12$, $^*P < 0.05$). (B) Inactivation rate constants (current decay after peak I_{Na}) were obtained by fitting the inactivating sodium current with a double exponential to obtain two rate constants: fast and slow component. R859H showed an overall slowing in the speed of inactivation, while the R865G only showed an increase in a slow inactivation rate constant (Student's *t*-test: $^*P < 0.05$, $^{**}P < 0.005$, $^{\dagger}P = 0.00095$; WT $n = 13$; R859H $n = 12$; R865G $n = 10$).

constant (τ_{slow}) of recovery (R859H $t_{10} = -2.81$, $P = 0.02$; R865G $t_{12} = -5.16$, $P = 0.0002$; Table 2).

Figure 3 illustrates the time to peak activation and the speed of inactivation for WT, R859H and R865G channels. We observed a significant delay in time to peak currents for R859H over the −30 to +5 mV voltage range, indicating a slowing in speed of activation of this mutant channel (Fig. 3A). To quantify the speed of sodium channel inactivation for WT, R859H and R865G channels, the decay in current traces during test pulses in the voltage range −30 to +30 mV were fitted with a double exponential to obtain fast and slow inactivation rate constants. The inactivation time constants were plotted against the test potentials (Fig. 3B). Rate constants corresponding to the fast component of inactivation were significantly larger in the voltage range of −20 to +10 mV for R859H, but not for R865G (Fig. 3B). The rate constant representing the slower component of inactivation for both mutations was significantly larger at many test potentials (Fig. 3B). These findings suggest impaired fast inactivation for both mutants.

Abnormal elevated persistent current can be generated by incomplete sodium channel inactivation during membrane depolarization and may facilitate repetitive action potential firing in neurons (Stafstrom, 2007). Previously certain $Na_v1.1$ mutations associated with GEFS+ and DS have been demonstrated to exhibit an increased persistent current (Lossin *et al.*, 2002; Rhodes *et al.*, 2004; Ohmori *et al.*, 2006). To analyze persistent current for R859H and R865G channels, we recorded sodium currents by applying 100 ms depolarizing pulses (from −120 to −20, −10 and 0 mV) in the absence or presence of tetrodotoxin, and digitally subtracted the currents.

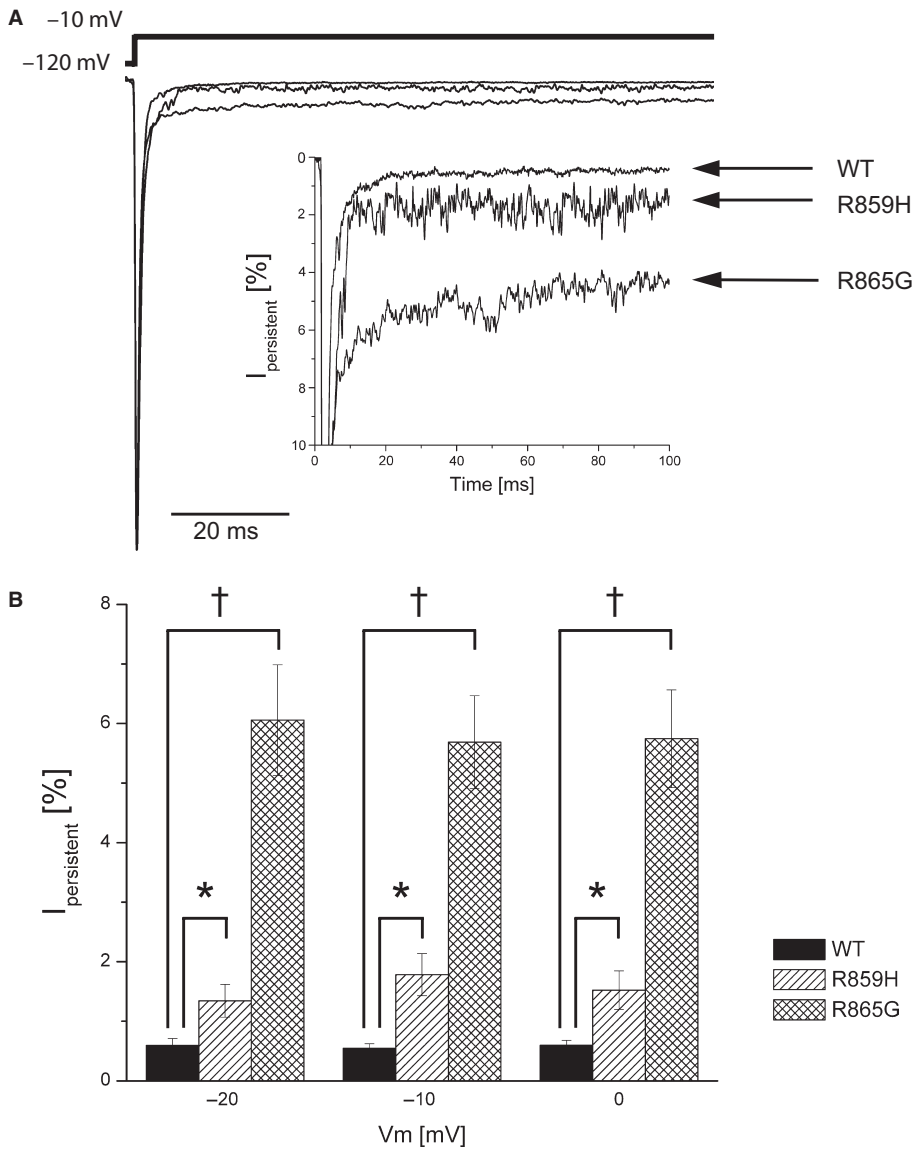

FIG. 4. Persistent current was increased in mutant channels. (A) Typical sodium current elicited by a long −10 mV depolarizing pulse. Persistent current was determined by a 100 ms depolarizing pulse from −120 mV to voltages −20, −10 and 0 mV. Tetrodotoxin-sensitive current recordings were obtained by digital subtraction of sodium currents before and after tetrodotoxin treatment. Persistent current was analyzed in the last 10 ms of the pulse and normalized to the peak sodium currents. Inset shows an expanded *y*-axis scaled to highlight the increased persistent current of R859H and R865G channels compared to WT. (B) The magnitude of persistent current as percentage of peak current amplitude plotted against the voltage steps. Both R859H and R865G mutants show a significant increase in persistent current at all test potentials, which suggest a destabilized inactivation gate that may lead to an increased hyperexcitability in neurons (Student's *t*-test: $*P < 0.05$, $^{\dagger}P < 0.001$; WT $n = 5$; R859H $n = 5$; R865G $n = 6$).

Persistent current was determined at the final 10 ms of the 100 ms depolarizing pulse and normalized to peak sodium currents. Both mutants exhibited a significantly increased persistent current compared to $Na_v1.1$ WT channels (Fig. 4). (−20 mV: R859H $t_8 = -2.51$, $P = 0.04$, $n = 5$; R865G $t_9 = -5.29$, $P = 0.0005$, $n = 6$; −10 mV: R859H $t_8 = -3.41$, $P = 0.009$, $n = 5$; R865G $t_9 = -5.95$, $P = 0.0002$, $n = 6$; 0 mV: R859H $t_8 = -2.27$, $P = 0.02$, $n = 5$; R865G $t_9 = -5.66$, $P = 0.0003$, $n = 6$).

Discussion

SCN1A mutations are linked to a spectrum of epileptic phenotypes, ranging in severity from GEFS+ to DS. For GEFS+ only missense mutations have been reported, leading to a wide array of biophysical gating defects. DS is often caused by mutations that are predicted to cause a truncated protein leading to a complete loss of function of the sodium ion channel. However, there are also several reports of missense mutations in patients with DS, some of which have been shown to produce functional ion channels *in vitro* (Rhodes *et al.*, 2004; Ohmori *et al.*, 2006).

We have studied four mutations in the *SCN1A* gene (R859H, R865G, R946C and R946H). Both R946C and R946H are associated with the Dravet phenotype and are mutations in the pore-loop region of the *SCN1A* gene. A few pore-loop mutations (R393H, H939Q, R946H, C959R and T1709I) have been functionally characterized and all mutations produced nonfunctional channels (Rhodes *et al.*, 2004; Ohmori *et al.*, 2006; Liao *et al.*, 2010). Our study also showed the pore-loop mutations (R946C and R946H) to be nonfunctional. Whether all pore-loop mutations are nonfunctional will require additional studies, but this finding is concordant with the general loss-of-function hypothesis of DS and supported by $Scn1a^{+/-}$ mice, which show that a reduction in sodium current in GABAergic inhibitory interneurons is sufficient to cause DS (Yu *et al.*, 2006; Ogiwara *et al.*, 2007; Catterall *et al.*, 2010).

Cells expressing the DIIS4 voltage sensor mutants R859H or R865G produced functional channels. Although both mutants produced sodium currents that were similar to WT currents, we also found various gating defects. For the GEFS+ mutant R859H we found a reduction in voltage-dependent steady-state channel availability and a delayed recovery from fast inactivation. However, this mutant also displayed an increased persistent current and slower inactivation rate constant, which may predispose a neuron to increased sodium conductance upon membrane depolarization. These data indicate that the mutant causes GEFS+ (including CPS) by mixed biophysical gating defects. Notably, effects differ from a previously reported GEFS+ mutant R859C, which showed smaller sodium peak currents, a depolarizing shift in the voltage dependence of activation, and a slower recovery from slow inactivation (Barela *et al.*, 2006). These discrepancies in results may be explained by the difference in amino acid substitution or differences in the experimental procedures such as the use of a *Xenopus* oocyte expression system instead of cultured human cells, expression of a mutated α-subunit in the absence of one of the β-subunits vs. a mutated α-subunit expressed with both $\beta 1$ and $\beta 2$-subunits, and a species-dependent modification of the rat vs. human $Na_v1.1$ channel. The DS mutant R865G showed predominantly gain-of-function defects, including a hyperpolarized shift in the voltage dependence of activation and a large increase in persistent current. Interestingly, the hyperpolarizing shift in the voltage dependence of activation observed for the R865G mutant, in combination with the unaltered voltage dependence of inactivation, indicates an increase in window current. The increased persistent current in both mutant channels is caused by an incomplete inactivation of the mutant channel, which leads to a proportion of channels either remaining open or to reopening (Kahlig *et al.*, 2006; Stafstrom, 2007). Previous studies of several *SCN1A* mutants associated with GEFS+ and DS (Lossin *et al.*, 2002; Rhodes *et al.*, 2004; Ohmori *et al.*, 2006) showed increased persistent current which may be a contributing factor to the complex epileptic phenotypes. However, the gain-of-function defects in the DS mutant R865G do not support the general loss-of-function hypothesis of DS (Catterall *et al.*, 2010), but the neuronal effects of these biophysical effects are not known.

It is not possible to extrapolate the gating defects of $Na_v1.1$ mutants to a neuronal network. In addition, the embryonic and postnatal development of the brains of subjects with *SCN1A* mutations, in combination with the genetic background, is difficult to determine. In this setting it seems feasible that any disturbance in excitation and inhibition in a neuronal network may lead to an epileptic outcome, including DS. There are reports of truncation mutations in *SCN1A* that lead to febrile seizures or GEFS+ instead of DS (Gennaro *et al.*, 2003; Yu *et al.*, 2010), indicating that the genetic background can play a role in the outcome of the disease. Such differences in severity of epileptic phenotypes have also been observed in $Scn1a^{+/-}$ mouse model strains (Yu *et al.*, 2006).

In this study further circumstantial evidence is provided that nonfunctional channels, as well as R865G mutant channels that show a variety of biophysical gating defects, can all cause DS. On the other hand, it can not be ruled out that mutant $Na_v1.1$ channels expressed in neurons behave differently than in our heterologous expression system, as tsA201 cells may lack key subunits of the ion channel macromolecular complexes. In neurons, defects in directing mutant $Na_v1.1$ proteins to the appropriate plasma membrane sites, e.g. soma or axon initial segment, might result in loss-of-function effects that can not be studied in tsA201 cells. Such distinct trafficking defects have been reported for sodium and potassium ion channel mutants (Mohler *et al.*, 2004; Chung *et al.*, 2006). In addition, fever-induced seizures are common in GEFS+ and DS subjects, and GEFS+ and DS mouse models showed increased seizure susceptibility at elevated body temperatures (Oakley *et al.*, 2009; Martin *et al.*, 2010). Future studies at physiological and febrile temperatures are warranted and could unmask important temperature-dependent gating effects.

Acknowledgements

This study was financially supported by the Ter Meulen Fund, Royal Netherlands Academy of Arts and Sciences, to L.V., the Netherlands Organization of Scientific Research and Development (ZonMW), VIDI grant number 917.66.315 to B.P.C.K., and the National Epilepsy Fund of the Netherlands (NEF 07-21) to M.v.K. and NIH grant NS032387 to A.L.G. None of the authors has any conflict of interest to disclose.

Abbreviations

CLZ, clonazepam; CPS, complex partial seizure; DS, Dravet syndrome; DTwcP-IPV, diphtheria/tetanus/whole cell pertussis/inactivated poliovirus; EEG, electroencephalography; GEFS+, genetic epilepsy with febrile seizures-plus; GTCS, generalized tonic–clonic seizures; Hib, haemophilus influenzae type b; LEV, levetiracetam; LTG, lamotrigine; TPM, topiramate; VPA, valproate; WT, wild-type.

References

Barela, A.J., Waddy, S.P., Lickfett, J.G., Hunter, J., Anido, A., Helmers, S.L., Goldin, A.L. & Escayg, A. (2006) An epilepsy mutation in the sodium

channel *SCN1A* that decreases channel excitability. *J. Neurosci.*, **26**, 2714–2723.

Berkovic, S.F., Harkin, L., McMahon, J.M., Pelekanos, J.T., Zuberi, S.M., Wirrel, E.C., Gill, D.S., Iona, X., Mulley, J.C. & Scheffer, I.E. (2006) De-novo mutations of the sodium channel gene *SCN1A* in alleged vaccine encephalopathy: a retrospective study. *Lancet Neurol.*, **5**, 488–492.

Catterall, W.A., Kalume, F. & Oakley, J.C. (2010) $Na_v1.1$ channels and epilepsy. *J. Physiol.*, **588**, 1849–1859.

Chung, H.J., Jan, Y.N. & Jan, L.Y. (2006) Polarized axonal surface expression of neuronal KCNQ channels is mediated by multiple signals in the KCNQ2 and KCNQ3 C-terminal domains. *Proc. Natl. Acad. Sci. USA*, **103**, 8870–8875.

Claes, L., Del-Favore, J., Ceulemans, B., Lagae, L., Van Broeckhoven, C. & De Jonghe, P. (2001) De novo mutations in the sodium-channel gene *SCN1A* cause severe myoclonic epilepsy of infancy. *Am. J. Hum. Genet.*, **68**, 1327–1332.

Depienne, C., Trouillard, O., Saint-Martin, C., Gourfinkel-An, I., Bouteiller, D., Carpentier, W., Keren, B., Albert, B., Gautier, A., Baulac, S., Arzimanoglou, A., Cazeneuve, W., Nabbout, R. & LeGeurn, E. (2009) Spectrum of *SCN1A* gene mutations associated with DS: analysis of 333 patients. *J. Med. Genet.*, **46**, 183–191.

Escayg, A., MacDonald, B.T., Meisler, M.H., Baulac, S., Huberfeld, G., An-Gourfinkel, I., Brice, A., LeGuern, E., Moulard, B., Chaigne, D., Buresi, C. & Malafosse, A. (2000) Mutation in *SCN1A*, encoding a neuronal sodium channel, in two families with GEFS+2. *Nature*, **24**, 343–345.

Fukuma, G., Oguni, H., Shirasaka, Y., Watanabe, K., Miyajima, T., Yasumoto, S., Ohfu, M., Inoue, T., Watanachai, A., Kira, R., Matsuo, M., Muranaka, H., Sofue, F., Zhang, B., Kaneko, S., Mitsudome, A. & Hirose, S. (2004) Mutations of neuronal voltage-gated Na+ channel alpha 1 subunit gene *SCN1A* in core severe myoclonic epilepsy in infancy (SMEI) and in borderline SMEI (SMEB). *Epilepsia*, **45**, 140–148.

Gennaro, E., Veggiotti, P., Malacarne, M., Madia, F., Cecconi, M., Cardinali, S., Cassetti, A., Cecconi, I., Bertini, E., Bianchi, A., Gobbi, G. & Zara, F. (2003) Familial severe myoclonic epilepsy of infancy: truncation of Nav1.1 and genetic heterogeneity. *Epileptic Disord.*, **5**, 21–25.

Harkin, L.A., McMahon, J.M., Iona, X., Dibbens, L., Pelekanos, J.T., Zuberi, S.M., Sadleir, L.G., Andermann, E., Gill, D., Farrell, K., Connolly, M., Stanley, T., Harbord, M., Andermann, F., Wang, J., Batish, S.D., Jones, J.G., Seltzer, W.K., Gardner, A., Infantile Epileptic Encephalopathy Referral Consortium, Sutherland, G., Berkovic, S.F., Mulley, J.C. & Scheffer, I.E. (2007) The spectrum of *SCN1A*-related infantile epileptic encephalopathies. *Brain*, **130**, 843–852.

Kahlig, K.M., Misra, S.N. & George, A.L. Jr (2006) Impaired inactivation gate stabilization predicts increased persistent current for an epilepsy-associated *SCN1A* mutation. *J. Neurosci.*, **26**, 10958–10966.

Liao, W.P., Shi, Y.W., Long, Y.S., Zeng, Y., Li, T., Yu, M.J., Su, T., Deng, P., Lei, Z.G., Xu, S.J., Deng, W.Y., Liu, X.R., Sun, W.W., Yi, Y.H., Xu, Z.C. & Duan, S. (2010) Partial epilepsy with antecedent febrile seizures and seizure aggravation by antiepileptic drugs: associated with loss of function of $Na_v1.1$. *Epilepsia*, **19**, 443–445.

Lossin, C. (2009) A catalog of *SCN1A* variants. *Brain Dev.*, **31**, 114–130.

Lossin, C., Wang, D.W., Rhodes, T.H., Vanoye, C.G. & George, A.L. Jr (2002) Molecular basis of an inherited epilepsy. *Neuron*, **34**, 877–884.

Lossin, C., Rhodes, T.H., Desai, R.R., Vanoye, C.G., Wang, D., Carniciu, S., Devinsky, O. & George, A.L. Jr (2003) Epilepsy-associated dysfunction in the voltage-gated neuronal sodium channel *SCN1A*. *J. Neurosci.*, **23**, 11289–11295.

Martin, M.S., Dutt, K., Papale, L.A., Dubé, C.M., Dutton, S.B., de Haan, G., Shankar, A., Tufik, S., Meisler, M.H., Baram, T.Z., Goldin, A.L. & Escayg, A. (2010) Altered function of the *SCN1A* voltage-gated sodium channel leads to gamma-aminobutyric acid-ergic (GABA-ergic) interneuron abnormalities. *J. Biol. Chem.*, **285**, 9823–9834.

Mohler, P.J., Rivolta, I., Napolitano, C., LeMaillet, G., Lambert, S., Priori, S.G. & Bennet, V. (2004) Nav1.5 E1053K mutation causing Brugada syndrome blocks binding to ankyrin-G and expression of Nav1.5 on the surface of cardiomyocytes. *Proc. Natl. Acad. Sci. USA*, **101**, 17533–17538.

Oakley, J.C., Kalume, F., Yu, F.H., Scheuer, T. & Catterall, W.A. (2009) Temperature- and age-dependent seizures in a mouse model of severe myoclonic epilepsy in infancy. *Proc. Natl. Acad. Sci. USA*, **106**, 3994–3999.

Ogiwara, I., Miyamoto, H., Morita, N., Atapour, N., Mazaki, E., Inoue, I., Takeuchi, T., Itohara, S., Yanagawa, Y., Obata, K., Furuichi, T., Hensch, T.K. & Yamakawa, K. (2007) Nav1.1 localized to axons of parvalbumin-positive inhibitory interneurons: a circuit basis for epileptic seizures in mice carrying an *Scn1a* gene mutation. *J. Neurosci.*, **27**, 5903–5914.

Ohmori, I., Kahlig, K.M., Rhodes, T.H., Wang, D.W. & George, A.L. Jr (2006) Nonfunctional *SCN1A* is common in severe myoclonic epilepsy of infancy. *Epilepsia*, **47**, 1636–1642.

Patino, G.A., Claes, L.R., Lopez-Santiago, L.F., Slat, E.A., Dondeti, R.S., Chen, C., O'Malley, H.A., Gray, C.B., Miyazaki, H., Nukina, N., Oyama, F., De Jonghe, P. & Isom, L.L. (2009) A functional null mutation of SCN1B in a patient with DS. *J. Neurosci.*, **29**, 10764–10778.

Rhodes, T.H., Lossin, C., Vanoye, C.G., Wang, D.W. & George, A.L. Jr (2004) Noninactivating voltage-gated sodium channels in severe myoclonic epilepsy of infancy. *Proc. Natl. Acad. Sci. USA*, **101**, 11147–11152.

Singh, R., Andermann, E., Whitehouse, W.P., Harvey, A.S., Keene, D.L., Seni, M.H., Crossland, K.M., Andermann, F., Berkovic, S.F. & Scheffer, I.E. (2001) Severe myclonic epilepsy of infancy: extended spectrum of GEFS+? *Epilepsia*, **42**, 837–844.

Spampanato, J., Escayg, A., Meisler, M.H. & Goldin, A.L. (2001) Functional effect of two voltage-gated sodium channel mutations that cause generalized epilepsy with febrile seizures plus type 2. *J. Neurosci.*, **21**, 7481–7490.

Spampanato, J., Esacyg, A., Meisler, M.H. & Goldin, A.L. (2003) Generalized epilepsy with febrile seizures plus type 2 mutations W1204R alters voltage-dependent gating of $Na_v1.1$ sodium channels. *Neuroscience*, **116**, 37–48.

Spampanato, J., Kearney, J.A., de Haan, G., McEwen, D.P., Escayg, A., Aradi, I., MacDonald, B.T., Levin, S.I., Soltesz, I., Benna, P., Montalenti, E., Isom, L.L., Goldin, A.L. & Meisler, M.H. (2004) A novel epilepsy mutation in the sodium channel *SCN1A* identifies a cytoplasmic domain for beta subunit interaction. *J. Neurosci.*, **24**, 10022–10034.

Stafstrom, C.E. (2007) Persistent sodium current and its role in epilepsy. *Epilepsy Curr.*, **7**, 15–22.

Suls, A., Claeys, K.G., Goossens, D., Harding, B., Van Luijk, R., Scheers, S., Deprez, L., Audenaert, D., Van Dyck, T., Beeckmans, S., Smouts, I., Ceulemans, B., Lagae, L., Buyse, G., Barisic, N., Misson, J.P., Wauters, J., Del-Favero, J., De Jonghe, P. & Claes, L.R. (2006) Microdeletions involving the *SCN1A* gene may be common in *SCN1A*-mutation-negative SMEI patients. *Hum. Mutat.*, **27**, 914–920.

Verbeek, N.E., van Kempen, M., Gunning, W.B., Renier, W.O., Westland, B., Lindhout, D. & Brilstra, E.H. (2011) Adults with a history of possible Dravet syndrome: an illustration of the importance of analysis of the SCN1A gene. *Epilepsia*, **52**, e23–e25.

Wallace, R.H., Wang, D.W., Singh, R., Scheffer, I.E., George, A.L. Jr, Philips, H.A., Saar, K., Reis, A., Johnson, E.W., Sutherland, G.R., Berkovic, S.F. & Mulley, J.C. (1998) Febrile seizures and generalized epilepsy associated with a mutation in the Na+ channel beta1 subunit SCN1B. *Nat. Genet.*, **19**, 366.

Yu, F.H., Mantegazza, M., Westenbroek, R.E., Robbins, C.A., Kalume, F., Burton, K.A., Spain, W.J., McKnight, G.S., Scheuer, T. & Catterall, W.A. (2006) Reduced sodium current in GABAergic interneurons in a mouse model of severe myoclonic epilepsy in infancy. *Nat. Neurosci.*, **9**, 1142–1149.

Yu, M.J., Shi, Y.W., Gao, M.M., Liu, X.R., Chen, L., Long, Y.S., Yi, Y.H. & Liao, W.P. (2010) Milder phenotype with *SCN1A* truncation mutation other than SMEI. *Seizure*, **19**, 443–445.